

High-Efficient Electric Power Converters Using Impedance Source Network

Nithyanantham.R¹, Vigneshwari.R²

PG Scholar, Department of EEE, Vandayar Engineering College, Thanjavur, India¹

Assistant Professor, Department of EEE, Vandayar Engineering College, Thanjavur, India²

Abstract— An Impedance network for electric power conversion to overcome the limitations and hazards faced by traditional converters such as voltage source, current source converter, various classical buck–boost, unidirectional, and bidirectional converter topologies. Impedance-source network with appropriate switching configurations and topologies reduces the number of power conversion stages in the system power chain. The impedance-source network overcomes the conceptual and theoretical barriers and limitations of the traditional VSI and CSI and provides a novel power conversion concept. The target of this new impedance network is to increase the boost, to reduce the number and size of both active and passive devices, to reduce the voltage stress on the active and passive devices, to improve the EMC of the system and to increase the reliability of the system. The impedance network improve the reliability, performance and reduces the harmonics of the system. Various analysis and designing process is done to overcome the problems by implementing the topology for various converters. In this impedance network various controller schemes are implemented to analyze the variation in the system and also to improve their performance and efficiency.

Index Terms— AC–AC power conversion, ac–dc power conversion, dc–ac power conversion, dc–dc power conversion, impedance source network.

I. INTRODUCTION-OVERVIEW

Impedance networks provide an efficient means of power conversion between source and load in a wide range of electric power conversion applications (dc–dc, dc–ac, ac–dc, ac–ac). Various topologies and control methods using different impedance-source networks have been presented in the literature, e.g., for adjustable-speed drives, uninterruptible power supply (UPS), distributed generation (fuel cell, photovoltaic (PV), wind, etc.), battery or super capacitor energy storage, electric vehicles, conversion with different switching cells. Distributed dc power systems, avionics, flywheel energy storage systems, electronic loads, dc circuit breaker and others. A variety of converter topologies with buck, boost, buck–boost, unidirectional, bidirectional, isolated as well as non isolated converters are possible by proper implementation of the impedance-source network with various switching devices, topologies, and configurations.

Fig. 1. General circuit configuration of impedance-source network for power The basic impedance-source network can be generalized as a two-port network with a combination of

two basic linear energy storage elements, i.e., L and C (dissipative components (R) are generally omitted). However, different configurations of the network are possible to improve the performance of the circuit by adding different nonlinear elements into the impedance network, e.g., diodes, switches, and/or a combination of both.

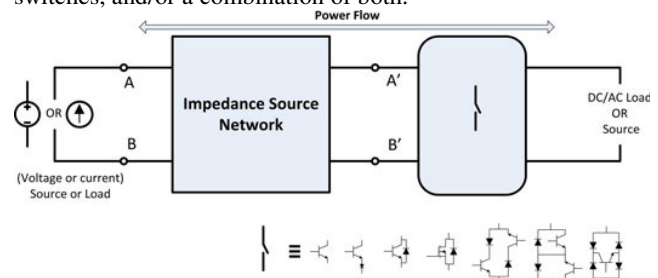


Fig. 1 shows the general configuration of an impedance-source network for electric power conversion, with possible switching configurations depending on application requirements.

The impedance-source network was originally invented to overcome the limitations of the voltage-source inverter (VSI) and current-source inverter (CSI) topologies which are commonly used in electric power conversion [1]–[5]. The ac output voltage of the VSI is limited below the input voltage, i.e., the VSI is a buck type inverter which cannot serve the need of distributed generation and ac drives alone. It requires an additional dc–dc boost converter to obtain a desired ac output, which increases system cost and lowers efficiency. In addition, the switching devices are vulnerable to electromagnetic interference as misgating on causes short-circuits across the inverter bridge and destroys the switching devices. The dead time introduced in such cases causes waveform distortion at the output. On the other hand, in the case of the CSI, the output voltage cannot be less than the input voltage. For applications where a wide voltage range is desirable, an additional dc–dc buck converter is needed. In addition, the upper and lower switches of the inverter have to be gated on and maintained on at any time. Otherwise, an open circuit of the dc inductor would occur and destroy the devices.

To utilize the properties of the impedance-source network, different switching configurations are being adopted and modulated with different pulse width modulation (PWM) and control techniques to match various application requirements. Possible switch configurations range from

simple-single switch topologies to very complex controlled multilevel and matrix configurations.

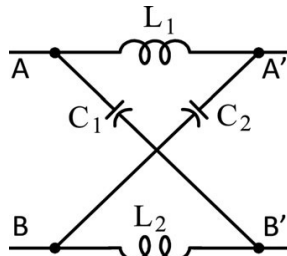


Fig. 2. Basic Z-Source impedance network.

The impedance-source converter overcomes the aforementioned conceptual and theoretical barriers and limitations of the classical VSI and CSI and provides a novel power-conversion concept. The major advantage of this topology is that it can operate as V -source or an I -source depending on the application and needs, and the output voltage can be varied from 0 to ∞ . Since the publication of the first impedance-source network, called a “Z-source network,” in year 2002 [1], many modified topologies with improved modulation and control strategies have been proposed and published to improve the performance in various applications. Fig. 2 shows the basic Z-source impedance network, which consists of inductors L_1 and L_2 and capacitors C_1 and C_2 connected at both ends (Z-shape) which acts as a buffer between load and source (voltage source or current source).

A. Operating Principle of the Impedance-Source Converter

The concept of the impedance-source network can be applied to any dc-to-dc, ac-to-ac, ac-to-dc, and dc-to-ac power conversions. The dc source and/or load can be a voltage or current source and/or a load. A Z-source impedance network is used as an example to briefly illustrate the operating principle and control of the impedance-source network. Fig. 3 shows the circuit diagram of the Z-source converter and its equivalent circuit during active and shoot-through states. During the shoot-through state, the output terminals of the impedance network A_- and B_- are short-circuited by a switch or combination of switches which will, in turn, cause diode D in the network to reverse-bias. Energy stored in the inductor and capacitor during this shoot-through state is transferred to the load during the next active state, in which the diode D is returned to conduction. The switching circuit viewed from the dc side during the active state is equivalent to a current source as shown in Fig. 3(a). Averaging of these two switching states results in an expression to compute the peak dc-link voltage $v_{A'_-B'}$, across terminals A' and B' , in terms of its input voltage V_{in} as $v_{A'_-,B'} = 1/(1-\beta d_{ST})V_{in} = \beta V_{in}$, where d_{ST} is the fractional shoot-through time assumed in a switching period, and $\beta \geq 2$ is a factor determined by the impedance network chosen, e.g., for Z-source inverter and quasi-Z-source inverter (ZSI and qZSI), $\beta = 2$. Equating the denominator of the boost factor (β) to zero then results in the permissible range of d_{ST} as $0 \leq d_{ST} < 1/\beta$, whose upper limit corresponds to an infinite gain. A

three-phase voltage-fed ZSI, as shown in Fig. 4, is used as an example to briefly illustrate the operating principle as described previously. The three-phase ZSI bridge has nine permissible switching states (six active states, two zero states, and one shoot-through state), unlike the traditional three-phase VSI which has eight (six active states, two zero states). During zero states, the upper three or lower three switches of the inverter bridge are turned on simultaneously, thus shorting the output terminals of the inverter and producing zero voltage across the load. During one of the six active states, the dc voltage is impressed across the load, positively or negatively. However, during shoot-through states, the load terminals are shorted through both the upper and lower devices of any one-phase leg, any two phase legs, and all three-phase legs [1] producing zero voltage across the load. This shoot-through state has the same effect, i.e., producing zero voltage across the load as the traditional zero states; however, these shoot-through states can boost the output voltage. The shoot-through state is forbidden in the traditional VSI, because it would cause a short circuit across the dc link and damage the converter. The Z-source network and the shoot-through zero state provide a unique buck-boost capability for the inverter by varying the shoot-through time period and modulation index M of the inverter. Theoretically, the output voltage of the inverter ($\hat{v}_{ac} = MB/2 = M[1 - 2d_{ST}]^{-1}V_{in}/2$) can be set to any value between 0 and ∞ . However, some practical aspects and performance of the converter need to be considered for large voltage buck or boost operation, e.g., to avoid exceeding device limitations. All the traditional PWM schemes can be used to control the impedance-source converter, and their theoretical input-output relationships still hold true. However, in addition to all states in the traditional modulation techniques, a new state called a “shoot-through state” is introduced and embedded in the modulation strategy for the impedance network-based power converter without violating the volt-sec balance in the operating principle. With the unique feature of these shoot-through states, several new PWM methods modified from sine PWM and space vector modulation are developed to control the output voltage. In addition, there is various control methods applied for various applications which will be discussed in Part II in detail.

B. Status of Impedance-Source Topologies and Applications

Z-source-related research has grown rapidly since it was first proposed in 2002; the numbers of modifications and new Z source topologies have grown exponentially. Fig. 5 shows the number of publications over the last ten years (a total of 1113 as of Sept. 2013) and a summary of the Z-source converter categories and Z-source network topologies that can be found in the recent literature. According to the conversion functionality, it can be divided into four main categories: dc-dc converters, dc-ac inverters, ac-ac converters, and ac-dc rectifiers. A further breakdown leads to two-level and multilevel, ac-ac and matrix converters, and non isolated and isolated dc-dc converters. From the Z-source network

topology standpoint, it can be voltage-fed or current-fed. Further, impedance networks can be divided based on the magnetic used in the impedance-source network, i.e., non transformer based and transformer or coupled inductor based.

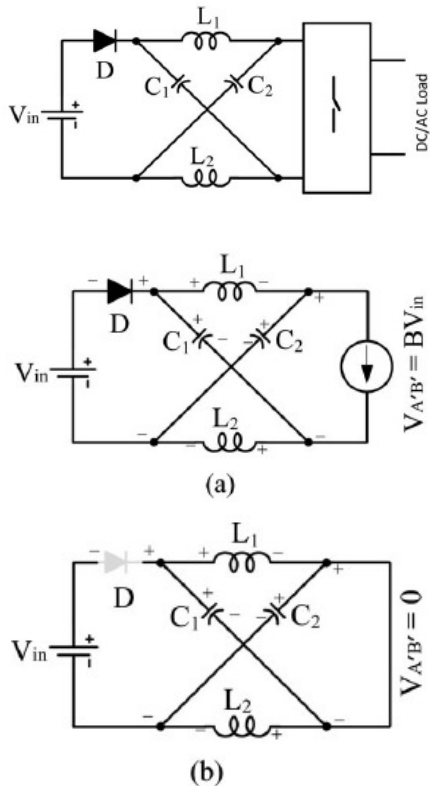


Fig. 3. Voltage-fed Z-source converter illustrating its equivalent circuit during (a) active state and (b) shoot-through state

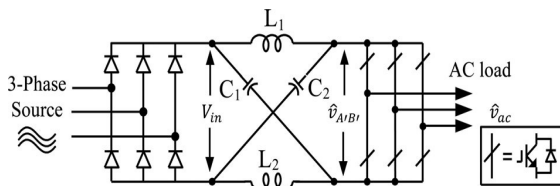


Fig. 4. Voltage-fed ZSI—an example of a ZSI

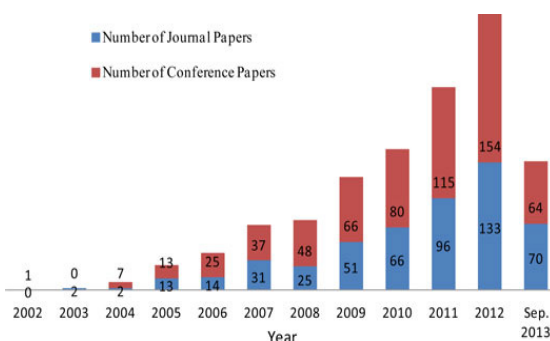


Fig. 5. Numbers of publications (total 1113 as of Sept. 2013).

The Z-source concept has opened up a new research area in power electronics. The previous description only provides a brief summary of the major Z-source network topologies. There are many modifications and variations on the previous Z-source topologies. Each topology has its own unique features and applications to which it is best suited. There is no one-size-fits-all solution. It is expected that new Z-source topologies will continuously be put forth to meet and improve converter performance in different applications. Renewable energy generation, such as PV and wind power, and motor drives are prospective applications of Z-source converters because of the unique voltage buck-boost ability with minimum component count and potential low cost. New power electronic devices, such as silicon carbide (SiC) and gallium nitride (GaN) devices, will definitely improve the performance of Z-source converters.

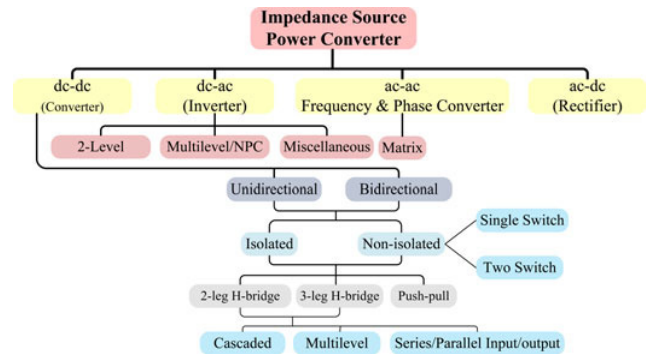


Fig. 6. Categorization of impedance-source network-based power converters.

Their high switching frequency, low loss, and high temperature capacity will contribute to small Z-source passive components, high efficiency of the converter, and high power density. Currently, Z-source converters are still advancing in topologies and applications.

C. Operating Principle

An impedance-source network can be generalized as a two port network with a combination of two basic passive linear elements, e.g., L and C (a dissipative component R is generally omitted). However, different derivations and modifications of the network are possible to improve the performance of the circuit by adding different nonlinear elements in the impedance network, e.g., diodes, switches, and/or a combination of both. The impedance-source network was originally invented to overcome the limitations of the voltage source inverter (VSI) and the current source inverter (CSI) topologies, which are mostly used in electric power conversion.

A three-phase voltage-fed Z-source inverter, as shown in Fig. 3(a), is used as an example to illustrate the operating principle. The traditional three-phase voltage-source inverter has six active states and two zero states. For the Z-source inverter, several extra shoot-through states are possible by gating on both the upper and lower devices of any one-phase

leg, any two-phase legs, or all three-phase legs [2]. Fig. 3(b) shows the basic modified carrier-based PWM control accommodating shoot-through states which are evenly distributed among the three-phase legs.

This shoot-through zero states are forbidden in the traditional voltage-source inverter, because they would cause a short circuit across the dc link. The Z-source network and the shoot through zero states provide a unique buck-boost feature of the inverter.

D. Modeling and Control

A Z-source network shows non minimum phase behavior due to the presence of zero in the right half-plane which could impose a limitation on the controller design. In order to implement a good control strategy, it is imperative to have a good dynamic model of the converter. Various small-signal analyses and mathematical models are presented in the literature to study the dynamic behavior of the system, which then can be implemented in different closed-loop control strategies with different complexities based on various applications.

To derive an accurate small-signal model, various state variables are selected, such as the input current ($i_{in}(t)$), inductor currents ($i_{L1}(t)$, $i_{L2}(t)$, . . .), capacitor voltages ($v_{C1}(t)$, $v_{C2}(t)$, . . .), and load currents ($i_L(t)$, $i_d(t)$, $i_q(t)$). The small-signal model provides the required transfer function for the controller design and provides a detailed view of the system dynamics, helps to understand the system limits, and provides guidelines for system controller design.

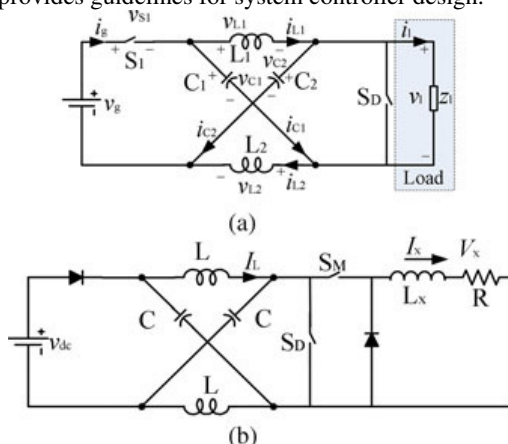


Fig. 7. Simplified equivalent circuit of Z-source converter for small-signal modeling: (a) D_{st} as control variable and (b) D_{st} and M as control variable.

In general, M and D_{st} are considered as control variables and the capacitor voltage ($v_C(t)$) or the dc-link voltage ($v_{PN}(t)$) and the load voltage ($v_x(t)$) as variables to be controlled. Fig. 4(a) shows the simplified Z-source converter model for small-signal analysis, where $v_C(t)$ is controlled using D_{st} as a control variable (control switch S_D). This is the most simplified model, however it does not guarantee tight control of $v_x(t)$, which requires an additional control variable M (control switch S_M) as shown in Fig. 7(b). In addition to the state variables, the parasitic resistance of the inductor r and the equivalent series resistance (ESR) of the capacitor R

also influence the dynamics of the impedance-source networks and hence are also considered during modeling of the converter to analyze the sensitivity of the circuit under parameter variations.

Based on some of the above state variables, several small signal models have been proposed for symmetric or asymmetric ZSI and qZSI. Considering the symmetry of the network (using $v_{C1}(t) = v_{C2}(t) = v_C(t)$ and $i_{L1}(t) = i_{L2}(t) = i_L(t)$), a simplified small-signal model is presented in [45] and [59] for ZSI, where the load current is represented by a constant current source. However, such a model describes only the dynamics of the impedance network and fails to describe the dynamics of the ac load. To overcome this disadvantage, a third-order model is presented in and using $v_{C1}(t) = v_{C2}(t) = v_C(t)$, $i_{L1}(t) = i_{L2}(t) = i_L(t)$ and $i_L(t)$ as state variables. In this model, the ac side of the inverter is referred to the dc side with RL load and taking its current as a third-state variable. A similar third-order small-signal model is presented in, which considers the dynamics of the input-side current. In this, the current-fed qZSI is analyzed using $v_C(t)$, $i_L(t)$, and $i_{in}(t)$ as state variables to demonstrate the transient response of the inverter during the motoring and regeneration modes of operation for application in electric vehicles. Subsequent fourth- and higher order small-signal models are also presented for inverters and rectifiers to better understand the dynamics of the input/output (load/source) and the impedance network. However, the complexity in formulating the small-signal model and the control-loop design increases with the increase in state variables. To simplify this, various assumptions (symmetry in impedance network, balanced load) and simplifications (representation of ac load/source by its equivalent dc load/source) are prevalent in the literature without loss of generality and changes to dynamic performance.

The state-space-averaged small-signal modeling provides a derivation of various control-to-output and disturbance-to-output transfer functions, which helps to predict the system dynamics under the influence of various parameter changes. The root locus of the control-to output transfer function in the s-domain gives a clear map of the converter dynamics. In addition, predicting a right-half-plane (RHP) zero in the control-to-output transfer function is a major advantage of small-signal modeling. The presence of RHP zeros indicates that the non minimum phase undershoot (the controlled capacitor voltage dips before it rises in response to a D_{st} increase), generally tends to destabilize the wide-band feedback loops, implying high gain instability and imposing control limitations. This means that the design of a feedback loop with an adequate phase margin becomes critical when RHP zeros appear in the transfer function. Various analyses of the pole-zero location and the impact of parameter variations on the converter dynamics are studied considering the wide operating ranges of different sources, e.g., fuel cells and photovoltaic's. Fig. 5 shows the locus of the poles and zeros with changes in various parameters such as L , C , D_{st} , R , and r .



The impact of parameter variations on the system dynamics as discussed above can provide direction to designers beforehand to choose component values while considering the design constraints, such as feedback control bandwidth, ripple content, size and cost of components, damping factor, resonant frequency, and overshoot/undershoot in the desired output. When considering the effect of parameter variations and the effect of poles and RHP zero, several closed-loop control methods are proposed in the literature to achieve a desired performance and to control the dc-link voltage and the ac output voltage of the impedance-source converter. In all these control methods, there are two control degrees of freedom (D_{st} and M).

II. GENERAL CLASSIFICATION OF MODULATION TECHNIQUES

Proper modulation of an impedance-source converter requires careful integration of the selective shoot-through process with the classical switching concepts to achieve maximal voltage boost, minimal harmonic distortion, low semiconductor stress, and a minimum number of devices commutations per switching cycle.

A. Modulation Techniques for Single -Phase Topologies

Various modulation techniques are presented in the literature to modulate and control the output voltage of single-phase impedance source inverters having two switches (semi-Z source, quasi-Z-source), four-switch intermediate H-bridge topologies, or embedded Z-source for different applications. A two-switch topology offers a simple and cost-effective solution for a single-phase grid-connected photovoltaic system. Two modulation techniques are prevalent in the literature to control and modulate the two switches of a single-phase Z-source/quasi-Z source to get the desired output voltage, namely one-cycle control and nonlinear sinusoidal pulse-width modulation (SPWM). The voltage gain of the semi-Z-source/quasi-Z-source converter is not a straight line as with a full-bridge inverter. So, instead of a sinusoidal reference signal ($v = V \sin \omega t$), a nonlinear sinusoidal reference signal $v = [2 - M \sin \omega t] - 1$ is compared with the carrier signal to generate the gate drive signal for the two switches as shown in Fig. 11(a). A similar modulation technique is also adopted in a single-phase embedded Z-source inverter with four switches. A one-cycle control method is adopted to control a single phase semi-Z-source topology in. In this control method, two switches work in a complementary fashion where the clock signal (CLK) is used to turn-on any one switch. The turn-on time of the switch is determined by the integrated voltage across the switch, and when it reaches the sinusoidal signal ($v_i - v_{ref}$), the integrator is reset and the switch turns OFF. This control method has the ability to reject input perturbations and is insensitive to the system model, which provides a high-efficiency constant-frequency control. A standard carrier-based PWM is modified in for a single phase H-bridge topology. A shoot-through state is placed instead of null state without altering the normalized volt-sec average voltage as shown in Fig. 11(c). The duration of each active state in a switching

cycle is kept the same as in the traditional SPWM. Therefore, the output waveforms are still sinusoidal; however, they are boosted to the desired level by properly controlling the Shoot-through time period. The paper extends the modulation concepts to the more complex three-phase H-bridge and four phase H-bridge topologies for a voltage-fed Z-source inverter in both continuous and discontinuous modes.

In addition to the above modulation and control method, a hysteresis-band current control is implemented in [88] for a H-bridge. The performance is tested for both symmetrical and asymmetrical Z-source networks. Similar to the modulation technique used in and for a three-phase inverter, a low-frequency harmonic-elimination PWM technique is implemented in for a single-phase inverter to reduce the output harmonic distortion and size of passive components found in the impedance network. Another cost-effective solution using two switches is presented in and is modulated by a conventional bipolar sinusoidal PWM technique. A saw tooth-carrier-based SPWM is also presented in for a single-phase module integrated inverter designed for a photovoltaic system. Compared to the conventional triangular-carrier-based method, this saw tooth-carrier method reduces the commutation times of the switches and helps to improve efficiency of the converter during the boost mode. This modulation method, strictly a carrier-based technique, together with other methods reviewed for single phase impedance network-based converters.

B. Modulation Techniques for Three Phase Topologies (2Level)

To date, several modified PWM control techniques for an impedance-source inverter have been proposed in the literature with the aim of achieving a wide range of modulation, less commutation per switching cycle, low device stress, and simple implementation. Modulation techniques for three-phase H-bridge topologies (2 levels) are broadly categorized as sine PWM (SPWM) and space-vector PWM (SVPWM). However, several other modifications can be found in the literature and will be discussed briefly as follows. SPWMs include simple boost control, maximum boost control, maximum constant boost control, and constant boost control with third-harmonic injection. A comparison of some of these SPWMs is presented in terms of the voltage gain. Simple boost control is the most basic and is derived from the traditional sinusoidal PWM where a carrier triangular signal is compared to the three-phase reference signal for sinusoidal output voltage and two straight lines (V_p and V_n) to create Fig. 8. Sine wave PWM (a) simple boost control, (b) maximum-boost control, (c) maximum-constant-boost control, and (d) constant-boost control with $1/6^{\text{th}}$ of third harmonic injection (\rightarrow Shoot-through period).

Shoot-through for voltage boost as shown in Fig. 8(a). The disadvantage of this modulation technique is a decrease of the modulation index with an increase of the shoot-through range. The maximum shoot-through duty ratio of the simple boost control is limited to D_{st} , $\max = (1 - M)$ which limits the boost factor to $B = [2M - 1] - 1$. As a result the device stress

increases for the application, which requires a higher voltage boost. To address this issue, a maximum-boost PWM control method is presented in [92]. This modulation technique maintains six active states unchanged from those of the traditional carrier-based PWM method; however, it utilizes all zero states to make shoot through states as shown in Fig. 8(b).

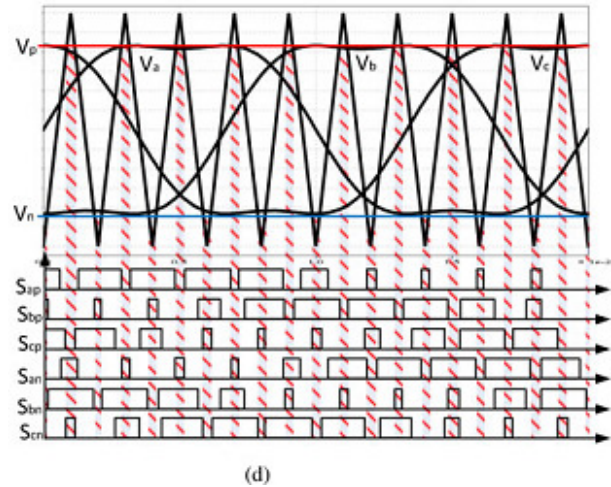
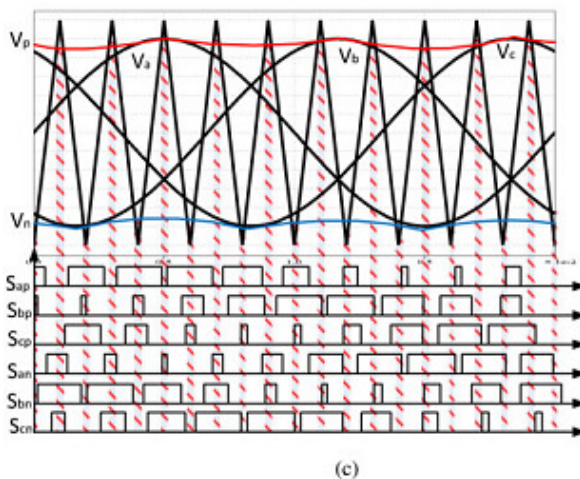
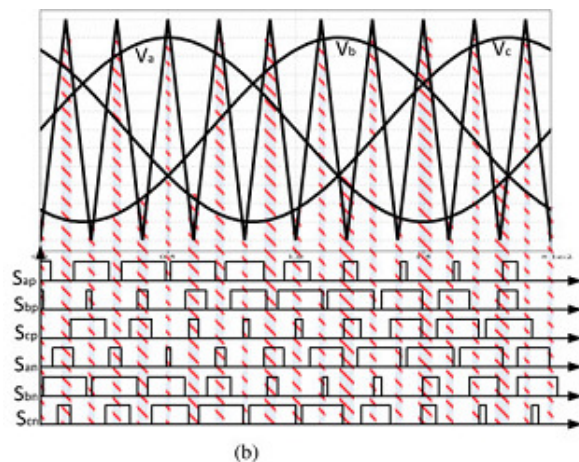
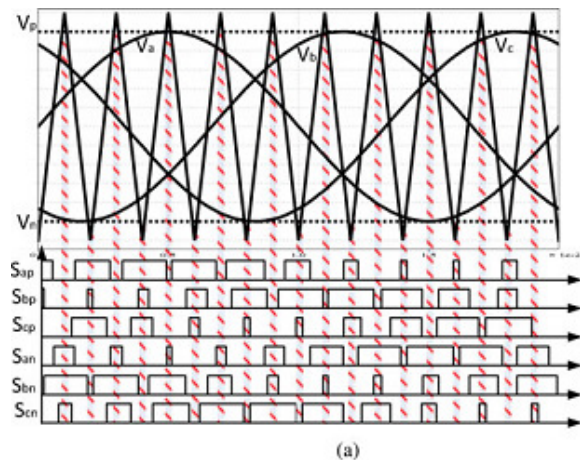


Fig. 8. Sine wave PWM (a) simple boost control, (b) maximum-boost control, (c) maximum-constant-boost control, and (d) constant-boost control with $1/6^{\text{th}}$ of third harmonic injection (\rightarrow Shoot-through period).

These increase the range of the boost factor $B = \pi [3\sqrt{3}M - \pi] - 1$ compared to using simple boost, which reduces the device stress. However, due to the variable shoot-through time intervals, low-frequency ripple components are present in the capacitor voltage and inductor current, which increases the size and cost of the components in the impedance network. To achieve a constant shoot-through duty ratio and a maximum boost factor, a maximum constant-boost PWM control method is proposed in and which eliminates the low-frequency harmonic component in the impedance-source network. Fig. 8(c) illustrates the switching waveforms of the maximum-constant-boost PWM control. The range of the modulation index is extended from 1 to $2/\sqrt{3}$ by injecting a third-harmonic component with $1/6$ of the fundamental component magnitude to the three-phase-voltage references. In this modulation technique, two straight lines V_p and V_n are required to generate a shoot-through time period as shown in Fig. 8(d). Besides SPWM, space vector pulse width modulation (SVPWM) has similarly been proven to be an effective modulation technique for traditional inverter topologies as it effectively reduces the commutation time of the switches, reduces the harmonic content in the output voltage/current, and better utilizes the dc-link voltage, and consequently reduces the voltage stress and switching loss. This benefit encourages researchers and engineers to retrofit SVPWM for various impedance source inverters. However, proper insertion of the shoot-through state in the switching cycle without altering the volt-sec balance is crucial to reduce additional commutation time of the switches and corresponding switching loss. A hybrid PWM strategy is subsequently proposed to reduce the algorithm calculation by combining the theory of SVPWM and triangular-comparison PWM for a three-phase-three-wire system and a three-phase-four-wire system. One cycle control similar to Fig. 11(b) is also proposed in for three-phase ZSI/qZSI using H-bridge switching topology. This is complemented by a



random PWM scheme proposed in for a Z-source inverter whose purpose is to reduce common mode voltage when used in an ac motor drive. For current fed qZSI, also proposes a modified SVPWM scheme for achieving higher input current utilization, lower switching loss, lower total harmonic distortion, and lower switching spikes across switching devices compared to traditional SVPWM. These advantages are attributed to the full-wave symmetrical modulation (FSM) applied whose outcome is only one short zero state vector ($_{17}$, $_{18}$, $_{19}$) utilized in each switching period

III. CONCLUSION

Impedance-source networks have added a new chapter in the field of power electronics with their unique features and properties that overcome most of the problems faced by traditional converter topologies. Since the publication of the first Z-source network, there have been numerous contributions in the literature modifying the basic topology to suit the needs of many applications. The impedance-source network overcomes the conceptual and theoretical barriers and limitations of the traditional VSI and CSI and provides a novel power conversion concept. The superior performance of the impedance-source network to design more robust and versatile converter topologies for various applications attracts researchers and designers from both academia and industry to explore it in depth. A close study of all the relevant topologies reveals that the modifications are motivated by one or more of the following reasons: 1) to increase the boost; 2) to reduce the number and size of both active and passive devices; 3) to reduce the voltage stress on the active and passive devices; 4) better input voltage (dc-link) utilization; 5) to improve the EMC of the system; and 6) to increase the reliability of the system, etc. In general, each individual topology may have a niche with targeted application(s), and it would not be possible to single out any particular circuit for general purposes. However, one may identify niche applications for particular networks that can improve the efficiency, reliability, and power density of the system and can fully utilize the potentials of new devices such as SiC and GaN. New application areas such as satellite, avionics, and medical are of special interest. The original Z-source network has been advanced to quasi-Zsource network, trans-Z-source network, distributed Z-source network, and many other types of Z-source network topologies. The original ZSI has been expanded to dc-dc, dc-ac, ac-dc, and ac-ac converters, respectively, in both two-level and multilevel structures with voltage- and current-fed from the power source. Over one thousand papers have been published and hundreds of Z-source converters have been proposed. In addition, each type (dc-dc, dc-ac, ac-dc, or ac-ac) of converter could potentially be implemented with the original Z-source

network, quasi-Z-source network, trans-Z-source, embedded Z-source, semi-Z-source, distributed Z-network, switched inductor Z source, tapped-inductor Z-source, diode-assisted Z-source, or capacitor-assisted Z-source. The number of combinations is large and the topologies are confusing. In this paper, in order to provide a global picture of the impedance source networks proposed in the literature, major Z-source network topologies have been surveyed and categorized based on conversion functionality and switching configurations. This survey and categorization help researchers to comprehend all these Z-source network topologies and PWM control schemes and targeted applications presented.

REFERENCES

- [1] F. Z. Peng, "Z-source inverter," in *Proc. Ind. Appl. Conf.*, Oct. 13–18, 2002, vol. 2, pp. 775–781
- [2] F. Z. Peng, "Z-source inverter," *IEEE Trans. Ind. Appl.*, vol. 39, no. 2, pp. 504–510, Mar./Apr. 2003.
- [3] F. Z. Peng, X. Yuan, X. Fang, and Z. Qian, "Z-source inverter for adjustable speed drives," *IEEE Trans. Power Electron.*, vol. 1, no. 2, pp. 33–35, Jun. 2003.
- [4] F. Z. Peng, A. Joseph, J. Wang, M. Shen, L. Chen, Z. Pan, E. O. Rivera, and Y. Huang, "Z-source inverter for motor drives," *IEEE Trans. Power Electron.*, vol. 20, no. 4, pp. 857–863, Jul. 2005.
- [5] Z. J. Zhou, X. Zhang, P. Xu, and W. X. Shen, "Single-phase uninterruptible power supply based on Z-source inverter," *IEEE Trans. Ind. Electron.*, vol. 55, no. 8, pp. 2997–3004, Aug. 2008.
- [6] A. Kulka and T. Undeland, "Voltage harmonic control of Z-source inverter for UPS applications," in *Proc. 13th Power Electron. Motion Control Conf.*, Sep. 1–3, 2008, pp. 657–662.
- [7] Y. Li, S. Jiang, J. G. Cintron-Rivera, and F. Z. Peng, "Modeling and control of quasi-Z-source inverter for distributed generation applications," *IEEE Trans. Ind. Electron.*, vol. 60, no. 4, pp. 1532–1541, Apr. 2013.
- [8] Y. P. Siwakoti and G. Town, "Performance of distributed DC power system using quasi Z-source inverter based DC/DC converters," in *Proc. Appl. Power Electron. Conf. Expo.*, Mar. 17–21, 2013, pp. 1946–1953.
- [9] B. Ge, H. Abu-Rub, F. Z. Peng, Q. Li, A. T. de Almeida, F. J. T. E. Ferreira, D. Sun, and Y. Liu, "An energy stored quasi-Z-source inverter for application to photovoltaic power system," *IEEE Trans. Ind. Electron.*, vol. 60, no. 10, pp. 4468–4481, Oct. 2013.

AUTHORS BIOGRAPHY



Nithiyantham.R received the Diploma from Government polytechnic College, Trichy (2007) in Electronics and Communication Engineering and B.E Degree from Periyar Maniammai University, Thanjavur(2012) in Electrical and Electronics Engineering and doing Master's Degree in Power Electronics and Drives from Vandayar Engineering College, Thanjavur, India. His area of Interest on Power Converters.